

The N-terminal domain of the replication initiator protein RepE is a dimerization domain forming a stable dimer[☆]

Akira Nakamura,^a Hirofumi Komori,^{a,1} Gengo Kobayashi,^b Akiko Kita,^a Chieko Wada,^b and Kunio Miki^{a,c,*}

^a Department of Chemistry, Graduate School of Science, Kyoto University, Sakyo-ku, Kyoto 606-8502, Japan

^b Institute for Virus Research, Kyoto University, Sakyo-ku, Kyoto 606-8507, Japan

^c RIKEN Harima Institute/Spring-8, Koto 1-1-1, Mikazuki-cho, Sayo-gun, Hyogo 679-5198, Japan

Received 29 December 2003

Abstract

The initiator protein RepE of the mini-F plasmid in *Escherichia coli* plays an essential role in DNA replication, which is regulated by the molecular chaperone-dependent oligomeric state (monomer or dimer). Crosslinking, ultracentrifugation, and gel filtration analyses showed that the solely expressed N-terminal domain (residues 1–144 or 1–152) exists in the dimeric state as in the wild-type RepE protein. This result indicates that the N-terminal domain functions as a dimerization domain of RepE and might be important for the interaction with the molecular chaperones. The N-terminal domain dimer has been crystallized in order to obtain structural insight into the regulation of the monomer/dimer conversion of RepE.

© 2004 Elsevier Inc. All rights reserved.

Keywords: Replication initiator; Dimerization domain; RepE; Mini-F plasmid; DnaK chaperone; Crystallization

Mini-F plasmid, a derivative of the F plasmid of *Escherichia coli*, is maintained at 1–2 copies per host chromosome, and the start of its replication is controlled by the RepE protein (251 residues, 29 kDa) encoded in the plasmid. This regulatory mechanism has been well studied [1,2]. RepE has dual functions according to its oligomeric state to control the number of plasmids strictly. The first function is that of a replication initiator factor mediated by the RepE monomers which bind to each of the four directly repeated DNA sequences (iterons) at the replication origin (*ori2*) to initiate the plasmid replication; the other function is that of an autogenous repressor mediated by the RepE dimer which binds to the operator of the *repE* gene to repress the transcription from the *repE* itself. The *repE* operator

contains an inverted repeat sequence related to an 8-bp region of the iteron. RepE proteins are mostly found as stable dimers and thus require host cell molecular chaperones (DnaK, DnaJ, and GrpE) to convert into RepE monomers, active forms as replication initiators [3,4] (C. Wada et al., unpublished data).

The crystal structure of the RepE mutant, RepE54 (R118P), which is a stable monomeric mutant with high initiator activity, has been determined as a complex with the iteron DNA [5]. The structure shows that RepE54 consists of a distinct N-terminal domain (residues 1–140) and C-terminal domain (residues 145–251). These domains are related to each other by an internal non-crystallographic 2-fold axis (Fig. 1). There are interactions between the major groove of iteron DNA and the helix–turn–helix motif of each domain, but the manner of protein–DNA interaction differs between the two domains. The N-terminal domain mainly contacts the phosphate backbone of DNA, whereas the C-terminal domain mainly interacts with DNA bases and plays the leading role in its DNA binding to the common sequence of 8 bases between the iteron and *repE*

[☆] Abbreviations: RepE NTD, N-terminal domain of RepE; His₆-RepE NTD, hexahistidine-tagged RepE NTD; RepE CTD, C-terminal domain of RepE; DSP, dithiobis[succinimidyl propionate].

* Corresponding author. Fax: +81-75-753-4032.

E-mail address: miki@kuchem.kyoto-u.ac.jp (K. Miki).

¹ Present address: Department of Structural Biology, Stanford University School of Medicine, Stanford, CA 94305, USA.

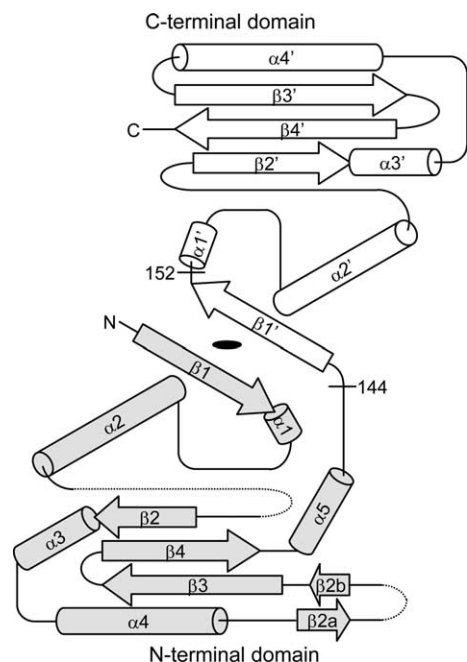


Fig. 1. Topology diagram of the RepE54 structure. The black ellipse indicates the pseudo-twofold axis relating the N-terminal (colored in gray) and C-terminal domains. The values 144 and 152 indicate the C-terminal cleavage positions of the construction for RepE NTD1 and NTD2, respectively.

operator. A hypothetical dimeric model of RepE based on the crystal structure of the RepE54 monomer suggests that the RepE N-terminal domain might be a dimerization interface and might require a large conformational change, especially in the step of monomer–dimer conversion. This is also supported by the genetical characterization of RepE mutants [6]. Biochemical and structural information about the dimerization process of RepE is indispensable in order to understand the molecular mechanism of the DNA replication regulation by RepE proteins. Here, we report the biochemical characterization of the N-terminal domain of RepE (hereafter RepE NTD), which is shown to function as a dimerization domain, and the preliminary X-ray characterization of the crystals of RepE NTD.

Materials and methods

Construction of the His₆-RepE NTD- and RepE NTD-overproducing plasmids. A DNA fragment encoding RepE NTD with a restriction digestion site at both ends was amplified from the plasmid pKV5110 [7] by the polymerase chain reaction (PCR) method using the primers containing the restriction enzyme recognition sequence, 5'-CGCGGATCCATGGCGGAAACAGCGGTTATC-3' (*Bam*HI) and 5'-CGTAAGCTTGTCTGTAAACCCGATAAAGAA-3' (*Hind*III). The amplified DNA fragment was digested with *Bam*HI and *Hind*III, and ligated to the *Bam*HI–*Hind*III-cut vector pKV7202 [8], which was constructed by deletion of the *Pvu*II–*Bal*I (*Msc*I) fragment from pQE-9 (Qiagen, Hilden, Germany). Construction of the non-His-tagged RepE NTD-overproducing plasmid was carried out using a method similar

to that for production of His₆-RepE NTD as described above. For RepE NTD1 (residues 1–144), PCR amplification was performed with the primers 5'-GCCACAGAATTCATTAAAGAGGAGAAATTA-3' (*Eco*RI) and 5'-CGTAAGCTTGTCTGTAAACCCGATAAAGAA-3' (*Hind*III), and the plasmid pKV7203 [8], the derivative of pKV7202, as a template. For RepE NTD2 (residues 1–152), a DNA fragment encoding residues 12–152 of RepE was amplified by PCR with the primers 5'-GCCGAATTCATGCGTAAAAATAGCCCGCGA-3' (*Eco*RI) and 5'-GGCAAGCTTCTAACTAAGCCGAAACTGCGT-3' (*Hind*III) and the template plasmid pKV7203, and then the fragment was ligated into the *Eco*RI–*Hind*III-cut pKV7203. The two plasmids, one encoding RepE residues 1–144 and the other encoding residues 12–152, were digested with *Sma*I and *Xba*I and ligated together to form a plasmid encoding residues 1–152 of RepE.

Construction of the His₆-RepE CTD-overproducing plasmid. Construction of the His₆-RepE CTD (C-terminal domain; residues 145–251)-overproducing plasmid was performed as described above for production of the overexpression plasmid of His₆-RepE NTD, with the exception that the PCR primers were 5'-CGCGGATCCCGGTTTACGAGTTTCGGCTT-3' (*Bam*HI) and 5'-CCGTAAGCTTCTATCCGTGTCGTCATGGAAGT-3' (*Hind*III).

Purification of RepE proteins. The constructed plasmid was transformed into M15 competent cell containing pRep-4 (Qiagen). Strain M15 cells, harboring the recombinant plasmid and pRep-4, were grown at 37°C in L broth [9] containing ampicillin and kanamycin (final concentrations of 50 and 25 µg ml⁻¹, respectively), and using these strains all RepE proteins were overexpressed severally. After induction of the expression of a RepE protein with 1 mM isopropyl β-D-thiogalactopyranoside (IPTG) for 4 h at 37°C, *E. coli* cells were harvested by centrifugation. All the His-tagged RepE proteins (His₆-RepE NTD, His₆-RepE, His₆-RepE54, and His₆-RepE CTD) were purified by the same procedure as that employed for His₆-RepE54 [10]. Purification of the RepE NTD proteins was carried out by the published procedure [1] with slight modifications. The harvested cells were sonicated in Buffer A (20 mM Tris–HCl, pH 7.5, 450 mM KCl, 0.1 mM EDTA, 10 mM β-mercaptoethanol, and 5.0 mM 4-(2-aminoethyl) benzensulfonyl fluoride (*p*-ABSF)) and centrifuged at 20,000g for 15 min. The crude extract was centrifuged at 150,000g for 1 h to remove host ribosomal proteins, and the supernatant was loaded onto a 50 ml SP-Toyopearl column (Tosoh, Tokyo, Japan) equilibrated with Buffer B (20 mM Mes–NaOH, pH 6.0, 200 mM KCl, and 0.1 mM EDTA). The column was eluted with a linear KCl gradient from 100 to 1000 mM, and then the eluates were concentrated, loaded onto a 320 ml Superdex column (Amersham Biosciences, Buckinghamshire, UK) equilibrated with Buffer C (50 mM potassium citrate, pH 6.2, 100 mM KCl), and eluted with the same buffer. Fractions containing the RepE NTD proteins were merged and stored at 4°C. Purified RepE proteins were more than 95% pure as estimated by sodium dodecyl sulfate–polyacrylamide gel electrophoresis (SDS–PAGE) followed by staining with Coomassie brilliant blue.

Crosslinking analysis. Crosslinking analysis of RepE proteins was performed as described previously [6]. The purified RepE proteins, His₆-RepE NTD, His₆-RepE, and His₆-RepE54, were crosslinked with dithiobis[succinimidyl propionate] (DSP) (Pierce, Rockford, IL) for 0, 15, or 30 min on ice and then the reactions were quenched. Non-crosslinked and crosslinked proteins were analyzed with SDS–PAGE (14%) followed by staining with silver.

Ultracentrifugation analysis. The purified RepE proteins, His₆-RepE NTD, His₆-RepE54, and His₆-RepE CTD, were dialyzed against Buffer C, and the concentrations were adjusted to 0.2 of absorbance at 280 nm. Then 110 µl of each protein solution was injected into one side of a 12-mm pathlength double-sector charcoal-filled Epon centerpiece, and the other side was injected with 125 µl of Buffer C. After the centerpieces were set in the An-60 Ti 4-place rotor, these samples were centrifuged at 15,000 rpm and 20°C in an Optima XL-I analytical ultracentrifuge (Beckman Coulter, Fullerton, CA). Sedimentation equilibrium analyses with the XL-I instrument were performed by

scans taken to measure the radial absorbance at 280 nm, while the baseline scans were taken to measure the absorbance at 280 nm toward Buffer C. Scans were taken at 2-h intervals after the initial 24-h centrifuge, and equilibrium was deemed to have been attained when the overlay of the consecutive scans showed no variation across the radial distribution. The collected scan data were analyzed using the Beckman software supplied with the centrifuge. Equilibrium absorbance distributions were fit to an ideal single species model following the equation below:

$$d(\ln A_r)/dr^2 = M(1 - v\rho)\omega^2/2RT, \quad (1)$$

where r is the radial position in the cell, A_r is the measured absorbance at the position r , M is the molecular weight of the protein, v is the partial specific volume of the protein, ρ is the solvent density, ω is the angular velocity, R is the universal gas constant, and T is the absolute temperature. The program SEDNTERP [11] was used to calculate the values of v based on amino acid composition (0.732, 0.733, and 0.728 ml g⁻¹ for His₆-RepE NTD, His₆-RepE54, and His₆-RepE CTD, respectively) and ρ at 20 °C (1.01 g ml⁻¹).

Gel filtration analysis. Five hundred microliters of solution containing 10 mg of purified RepE NTD1 with four molecular weight markers (bovine serum albumin, 67 kDa; hen egg ovalbumin, 43 kDa; bovine pancreas chymotrypsinogen A, 26 kDa; and bovine pancreas ribonuclease A, 14 kDa) for reference was loaded onto a size-exclusion Hi-Load 16/60 Superdex200 column (Amersham Biosciences) equilibrated with Buffer C. These proteins were eluted with the same buffer at a flow rate of 0.8 ml min⁻¹ (AKTA explorer 100 system) at room temperature. The elution pattern was monitored by measuring the absorbance at 280 nm.

Crystallization and X-ray diffraction. Crystallization was performed by the sitting-drop vapor-diffusion method at 20 °C using the protein solution containing 20 mg ml⁻¹ RepE NTD in Buffer C. Initial screenings to determine the crystallization conditions were carried out using commercially available screening kits (Hampton Research, Laguna Niguel, CA). During all the experiments, crystallizing drops containing equal volumes of the protein solution and precipitant solution were equilibrated against the precipitant solution. X-ray diffraction experiments were performed with crystals frozen under a cryo-nitrogen stream. Intensity data were collected using synchrotron radiation at beamlines BL41XU, BL38B1, and BL44B2 of SPring-8 (Harima, Japan) and at BL-6A of the Photon Factory (Tsukuba, Japan) with MARCCD165 and ADSC Quantum 4R as detectors. The X-ray wavelength, crystal-to-detector distance, and oscillation range were set to 1.0000 Å, 250 mm, and 1.0°, respectively. The image data were processed with the program package HKL-2000 [12].

Results and discussion

Preparation of RepE NTD

In the designing of a RepE NTD construction to elucidate the structure of the RepE dimer, clarification of the crystal structure of RepE54 was considered useful to determine the C-terminal cleavage point. RepE54 can be separated into N- and C-terminal domains at the loop (residues 141–144) between $\alpha 5$ and $\beta 1'$ (Fig. 1), and the N-terminal domain has most of the mutation sites found in dimerization defective mutants [6]. Moreover, each domain is a functional unit for binding to DNA by itself; in particular, the C-terminal domain recognizes the specific DNA sequence. Since there are common sequences of DNA between the iteron and the inverted

repeat of the operator, which must be recognized and bound by the C-terminal domain of RepE, assuming that the three-dimensional structure and the function of the C-terminal domain are not changed between the monomer and dimer, the dimerization of RepE is expected to occur in the N-terminal domain. Therefore, we employed residues 1–144 or 1–152 of RepE as RepE NTD (NTD1 or NTD2, respectively; Fig. 1), which is a potential dimer.

Examination for dimeric state

The oligomeric state of RepE NTD was examined by crosslinking, ultracentrifugation, and gel filtration experiments.

Crosslinking analysis

In a previous study, the dimer of RepE proteins was detected in the retained dimeric state on SDS-PAGE after chemical crosslinking using DSP, an NHS-ester crosslinker which covalently crosslinks two primary amines of mainly lysine residues in proteins [6]. In this analysis, all the RepE proteins were detected as monomers on SDS-PAGE before crosslinking. It was found that the His₆-Rep54 protein was not crosslinked with DSP, because the protein showed only a single band of 31 kDa monomers (label M in Fig. 2) after 30 min of incubation. On the other hand, the strength of the bands on SDS-PAGE corresponding to the dimers of His₆-RepE NTD and His₆-RepE (36 and 62 kDa, respectively, shown by the letter D in Fig. 2) was increased with time after addition of DSP. Furthermore, no products corresponding to a trimer or a larger oligomer

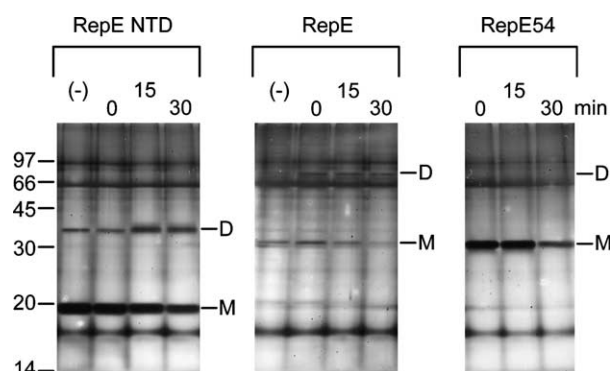


Fig. 2. SDS-PAGE patterns showing crosslinking of RepE proteins with DSP. The proteins (His₆-RepE NTD, His₆-RepE, and His₆-RepE54) and reaction mixtures were added to the sample loading buffer, subjected to SDS-PAGE, and analyzed by standard silver staining. D and M indicate the dimer and monomer positions, respectively. (–) indicates the lane of non-crosslinked protein. The values 0, 15, and 30 indicate the reaction time (minutes) of crosslinking. Relative positions of the molecular weight markers (kDa) are shown on the left.

were detected. These results indicate that RepE NTD forms a dimer just as the wild-type RepE does.

Ultracentrifugation analysis

The molecular weight was determined by the sedimentation equilibrium method. His₆-RepE NTD, His₆-RepE54, and His₆-RepE CTD were centrifuged at 15,000 rpm for 40 h at 20 °C, and scan data were collected at this time point. The data were fit to an ideal single species model (Fig. 3), and then by means of Eq. (1) the molecular weight of His₆-RepE NTD and His₆-RepE54 were calculated to be 34.5 and 32.1 kDa, respectively. As the molecular weights of His₆-RepE NTD predicted from the DNA sequence is 18.2 kDa, His₆-RepE NTD naturally exists in the dimeric state. In contrast, the molecular weight of His₆-RepE CTD was not estimated since an appropriate gradient of protein molecules could not be formed in the cell at this speed, which means the molecular weight of His₆-RepE CTD (14.3 kDa from DNA sequence) is approximately less than 28 kDa. This suggests that His₆-RepE CTD is a monomer.

Gel filtration analysis

In order to estimate the molecular weight of RepE NTD dependent on its shape, RepE NTD1 and marker proteins were subjected to gel filtration chromatography simultaneously. Elution position of RepE NTD1, which was highly the same as that of ovalbumin, was 84.1 ml after sample application. On the purification step under

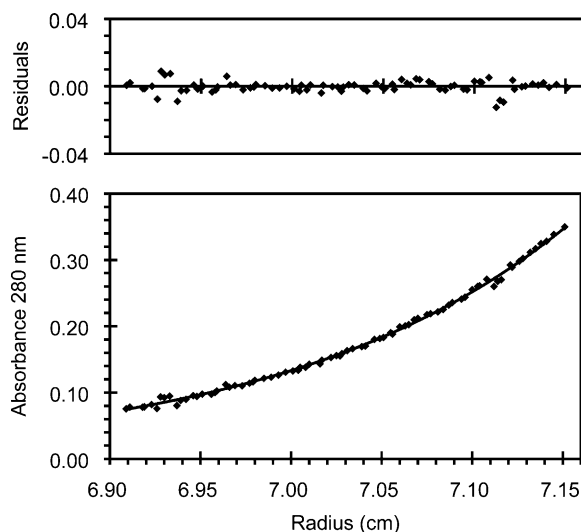


Fig. 3. Ultracentrifugation analysis of RepE NTD. The sedimentation equilibrium profile of His₆-RepE NTD after 40-h centrifugation at 15,000 rpm. Data are plotted as the absorbance at 280 nm versus the radial distance and are overlaid with the best-fit curve for a single species model. The distribution of the residuals is displayed above the experimental profile.

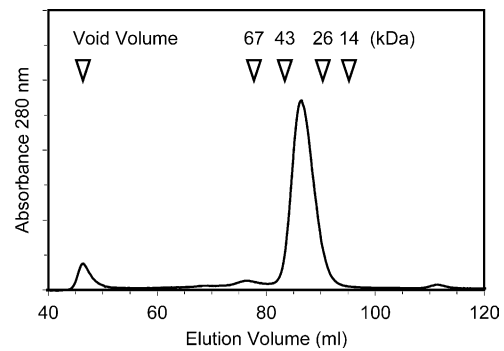


Fig. 4. Gel filtration analysis of RepE NTD. The elution pattern of RepE NTD1 is drawn with absorbance at 280 nm against eluted volume. The peak positions of molecular weight markers and the position of void volume are indicated at the top of the figure.

the same condition, the peak of RepE NTD1 elution occurred at 86.3 ml after loading; this peak was located between those of ovalbumin and chymotrypsinogen A. This elution pattern and the peak positions of the markers are exhibited in Fig. 4. Using a standard curve obtained with the reference proteins, the molecular weight of RepE NTD1 was estimated to be 33.1 kDa. This result implies that RepE NTD1 forms a stable dimer. With respect to RepE NTD2, its dimeric state was confirmed by gel filtration under the same conditions as for RepE NTD1. RepE NTD2 was eluted at almost the same position as RepE NTD1, indicating that RepE NTD2 is also present as a dimer.

Properties of RepE NTD

Three experiments demonstrated that RepE NTD, like the wild-type RepE, is stable as a dimer. RepE NTD2 (Fig. 1), which was expanded by the C-terminal eight residues from RepE NTD1, also showed the same feature. Basically, the N-terminal domain of RepE might carry a significant role in dimerization. In addition, the solely expressed RepE NTD constructed in this report was highly soluble to its maximum concentration of more than 100 mg ml⁻¹ in Buffer C, in contrast to the wild-type RepE, which aggregates easily at low concentration. Its solubility was still higher than that of RepE54 [5]. This drastic alteration of property might be caused by deletion of the C-terminal domain and by conformational change in the N-terminal domain between the monomer (RepE54) and dimer (RepE NTD), which would reduce an exposed hydrophobic region and form the dimer interface. The former is supported by the fact that RepE CTD shows a tendency to aggregate compared with RepE NTD (data not shown). The latter is supported by the presence of the predicted DnaK binding site in the N-terminal domain. Based on a previously reported algorithm [13], it is anticipated that DnaK could interact in particular with the α 2 helix and

the $\beta 3$ – $\beta 4$ – $\alpha 5$ region (named in the RepE54 structure). In addition, chaperone-independent copy-up mutations of RepE were located in the $\beta 3$ – $\beta 4$ – $\alpha 5$ region [6]. When the RepE dimer converts to a monomer, DnaK and its co-chaperones might interact with the hydrophobic region and promote the dimer–monomer conversion while preventing the aggregation of proteins. These characterizations in the RepE protein were supported by the structural information of the homologous protein RepA, in which a significant conformational change was observed in a similar dimerization domain [14].

Crystallization

Plate-like shaped crystals of RepE NTD1 and prismatic crystals of RepE NTD2 were obtained from the condition I (16.0% (w/v) polyethylene glycol (PEG) 4000, 18.0% (v/v) 2-propanol, and 100 mM Hepes–NaOH, pH 7.0) and condition II (9.6% (w/v) PEG 4000, 9.2% (v/v) 2-propanol, and 100 mM potassium citrate, pH 6.2), respectively (Fig. 5). In X-ray diffraction experiments, the crystals of RepE NTD1 and NTD2 were soaked in cryoprotectant solutions I (35.0% (w/v) PEG 4000, 10.0% (v/v) 2-propanol, and 100 mM potassium citrate, pH 6.2) and II (12.0% (w/v) PEG 4000, 9.0% (v/v) 2-propanol, 25.0% (v/v) ethylene glycol, and 100 mM potassium citrate, pH 6.2), respectively, and

then flash-cooled under the cryosystem. Diffractions from the crystals were extended beyond 4 Å resolution. The crystal of RepE NTD1 belongs to the monoclinic space group $C2$, with the unit cell parameters of $a = 128.2$ Å, $b = 57.5$ Å, $c = 113.6$ Å, and $\beta = 118.3^\circ$. The crystal of RepE NTD2 also belongs to the space group $C2$, with the unit cell parameters of $a = 205.7$ Å, $b = 83.5$ Å, $c = 71.2$ Å, and $\beta = 106.4^\circ$. Assuming two dimers of RepE NTD1 or three dimers of RepE NTD2 per asymmetric unit, the Matthews coefficient, V_M , and the solvent content are estimated to be 2.8 Å³ Da^{−1} and 56% for both crystals [15]. Both the datasets for RepE NTD1 and NTD2 were collected up to 3.8 and 4.1 Å resolution, respectively. As many as 6792 and 7753 of unique (27,215 and 32,625 of total) reflections ($I > 1\sigma(I)$) were obtained with 90.1% (76.1%) and 84.5% (59.4%) of completeness and 0.086 (0.302) and 0.050 (0.314) of R_{sym} for RepE NTD1 and NTD2, respectively, where $R_{\text{sym}} = \sum_{hkl} |I - \langle I \rangle| / \sum_{hkl} I$ and the values of the highest resolution shell are given in parentheses for completeness and R_{sym} . The fact that the preliminary molecular replacement using the structure of the N-terminal domain (residues 15–144) of the RepE54–iteron complex (Protein Data Bank code 1REP) [5] as a search model gave no effectual solutions might have been due to large structural differences between the N-terminal domain of RepE54 and RepE NTD.

In conclusion, the N-terminal domain could be assigned as a dimerization domain of RepE, whereas the C-terminal domain was shown to be a sequence-specific DNA binding domain. The conversion mechanism of RepE from dimer to monomer based on the structural information would be revealed in detail by the crystal structure determination of RepE NTD.

Acknowledgments

We thank Drs. M. Kawamoto, H. Sakai, K. Miura, and S. Adachi of SPring-8 (Proposal Nos. 2002B0393-NL1-np and 2002B0848-RL1-np) and Drs. M. Suzuki and N. Igarashi of the Photon Factory (Proposal No. 2003G131) for their help with the X-ray diffraction experiments. K.M. is a member of the Structural Biology Sakabe Project of the Photon Factory. This work was supported by a Grant-in-Aid for Scientific Research on Priority Areas and a grant of the National Project on Protein Structural and Functional Analyses from the Ministry of Education, Culture, Sports, Science and Technology of Japan.

References

- [1] M. Ishiai, C. Wada, Y. Kawasaki, T. Yura, Replication initiator protein RepE of mini-F plasmid: functional differentiation between monomers (initiator) and dimers (autogenous repressor), *Proc. Natl. Acad. Sci. USA* 91 (1994) 3839–3843.
- [2] H. Uga, F. Matsunaga, C. Wada, Regulation of DNA replication by iterons: an interaction between the *ori2* and *incC* regions mediated by RepE-bound iterons inhibits DNA replication of

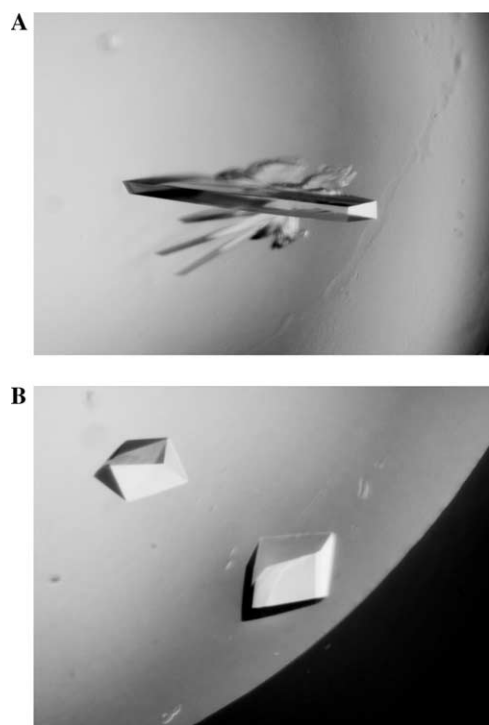


Fig. 5. Crystals of the RepE N-terminal domains. (A) Crystals of RepE NTD1 with approximate dimensions of $0.4 \times 0.1 \times 0.05$ mm for the biggest one of the cluster. (B) Crystals of RepE NTD2 with approximate dimensions of $0.3 \times 0.15 \times 0.15$ mm.

- mini-F plasmid in *Escherichia coli*, EMBO J. 18 (1999) 3856–3867.
- [3] Y. Kawasaki, C. Wada, T. Yura, Roles of *Escherichia coli* heat shock proteins DnaK, DnaJ and GrpE in mini-F plasmid replication, Mol. Gen. Genet. 220 (1990) 277–282.
- [4] Y. Kawasaki, C. Wada, T. Yura, Binding of RepE initiator protein to mini-F DNA origin (*ori2*). Enhancing effects of *repE* mutations and DnaJ heat shock protein, J. Biol. Chem. 267 (1992) 11520–11524.
- [5] H. Komori, F. Matsunaga, Y. Higuchi, M. Ishiai, C. Wada, K. Miki, Crystal structure of a prokaryotic replication initiator protein bound to DNA at 2.6 Å resolution, EMBO J. 18 (1999) 4597–4607.
- [6] F. Matsunaga, M. Ishiai, G. Kobayashi, H. Uga, T. Yura, C. Wada, The central region of RepE initiator protein of mini-F plasmid plays a crucial role in dimerization required for negative replication control, J. Mol. Biol. 274 (1997) 27–38.
- [7] Y. Kawasaki, C. Wada, T. Yura, Mini-F plasmid mutants able to replicate in the absence of σ^{32} : mutations in the *repE* coding region producing hyperactive initiator protein, J. Bacteriol. 173 (1991) 1064–1072.
- [8] F. Matsunaga, Y. Kawasaki, M. Ishiai, K. Nishikawa, T. Yura, C. Wada, DNA-binding domain of the RepE initiator protein of mini-F plasmid: involvement of the carboxyl-terminal region, J. Bacteriol. 177 (1995) 1994–2001.
- [9] C. Wada, Y. Akiyama, K. Ito, T. Yura, Inhibition of F plasmid replication in *htpR* mutants of *Escherichia coli* deficient in sigma 32 protein, Mol. Gen. Genet. 203 (1986) 208–213.
- [10] H. Komori, N. Sasai, F. Matsunaga, C. Wada, K. Miki, Crystallization and preliminary X-ray diffraction studies of a replication initiator protein (RepE54) of the mini-F plasmid complexed with iteron DNA, J. Biochem. 125 (1999) 24–26.
- [11] T.M. Laue, B.D. Shah, T.M. Ridgeway, S.L. Pelletier, Computer-aided interpretation of analytical sedimentation data for proteins, in: S.E. Harding, A.J. Rowe, J.C. Horton (Eds.), Analytical Ultracentrifugation in Biochemistry and Polymer Science, Royal Society of Chemistry, Cambridge, 1992, pp. 90–125.
- [12] Z. Otwinowski, W. Minor, Processing of X-ray diffraction data collected in oscillation mode, in: C.W. Carter, R.M. Sweet (Eds.), Volume 276: Macromolecular Crystallography, part A, Methods in Enzymology, Academic Press, New York, 1997, pp. 307–326.
- [13] S. Rudiger, L. Germeroth, J. Schneider-Mergener, B. Bukau, Substrate specificity of the DnaK chaperone determined by screening cellulose-bound peptide libraries, EMBO J. 16 (1997) 1501–1507.
- [14] R. Giraldo, C. Fernández-Tornero, P.R. Evans, R. Díaz-Orejas, A. Romero, A conformational switch between transcriptional repression and replication initiation in the RepA dimerization domain, Nat. Struct. Biol. 10 (2003) 565–571.
- [15] B.W. Matthews, Solvent content of protein crystals, J. Mol. Biol. 33 (1968) 491–497.